CCIT Report #521 March 2005

A Spurious-Free Source-Model Technique for Waveguide Mode Determination

Amit Hochman and Yehuda Leviatan

March 16, 2006

Abstract

Some difficulties in the application of source-model techniques to waveguide mode determination are pointed out, and shown to stem from approximate spurious solutions to the characteristic equation of the waveguide. An approach that avoids these spurious solutions is presented, yielding a method more reliable and efficient.

1 Introduction

The Source-Model Technique (SMT) can be classified as a Method of Moments (MoM), where the fields of discrete sources, located a distance away from the boundaries, are used to approximate the fields (see [1] for a review). This is in contradistinction to the probably more common, surface-formulations, that employ continuous sources coincident with the boundaries. The SMT has been applied to a wide range of scattering problems and is known in this context also by many other names: "Method of Auxiliary Sources" [1], "Generalized Multipole Technique" [2], "Method of Fundamental Solutions" [3], and so on. Simplicity of implementation, high numerical accuracy and stability, make the SMT a viable alternative to the surface-formulations.

Since waveguide mode determination can be thought of as a scattering problem with vanishing excitation, it is natural to assume that the SMT can be applied to it straightforwardly. The literature on this subject, however, is quite scarce. Indeed, only recently has the SMT been used to calculate the modes of an elliptical metallic waveguide [3].

Although the SMT is a powerful method for waveguide mode determination, we will show that the existence of spurious solutions can hinder its practical application considerably.

This letter is organized as follows: Section 2 outlines the essentials of the SMT and describes how the existence of spurious solutions in the SMT formulation renders the determination of modal solutions problematic. Section 3 explains the problematic behavior by use of an analytic approximation of the spurious solutions. Section 4 presents the proposed remedy, together with a

numerical example that demonstrates its effectiveness. The last section is a summary.

2 Problem Description

The problem we describe exists in a SMT analysis of a general cylindrical waveguide consisting of piecewise homogeneous material which may be bounded by perfect electric conductors. The approach presented is directly applicable to the general geometry, and in fact, we have used it successfully in the analysis of complex photonic-crystal fibers [4]. To avoid cluttering the presentation with nonessential detail, we will focus on using the SMT to calculate the well-known transverse-magnetic (TM) modes of a circular metallic waveguide. This also allows us to explain the method more clearly by using an analytic approximation of the fields due to the sources. It is worth emphasizing that this is only an explanatory device and does not compromise the generality of the method.

In the SMT, TM modes are approximated by the fields of an array of N electrical current filaments, uniformly distributed on a circle outside the waveguide, concentric with the waveguide. The filaments carry a longitudinally varying current, whose dependence on the longitudinal coordinate z, for $\exp(j\omega t)$ time dependence, is $\exp(-j\beta z)$. A factor of $\exp(j\omega t - j\beta z)$ will be therefore assumed and suppressed throughout. We denote the waveguide radius by R. The radius of the circle on which the sources are located is larger than R by a factor α ($\alpha > 1$). The amplitudes of the sources are arranged in an N-tuple column vector, denoted by $\vec{I}$. These amplitudes are found by requiring the longitudinal electric field, E_z, to be zero at a set of M testing points, uniformly distributed on the waveguide circumference. This leads to a homogeneous matrix equation

$$[Z]\vec{I} = \vec{0}, \tag{1}$$

where $[Z]$ is the $M \times N$ impedance matrix. More testing points than sources are generally used to ensure that the boundary conditions are obeyed more uniformly along the boundary. Throughout this work, we used twice as many testing points as sources, so $M = 2N$. These are the essentials of the SMT, needed to describe the spurious-solutions problem. Further details regarding the implementation of the SMT up to this point can be found in [5].

Equation (1) has nontrivial solutions if and only if $[Z]$ is singular, or as is the case in any approximate numerical solution, close to singular. To find the modes, a suitable measure of the singularity of $[Z]$ must be chosen and evaluated at the relevant values of the radial wave number, k_ρ, which is related to β and ω by the separation equation

$$k_\rho = \sqrt{(\omega/c)^2 - \beta^2}, \tag{2}$$

where c is the speed of light *in vacuo*. A common measure of singularity, and the one we employ here is the condition number of $[Z]$. Other measures that have been used are the closely related, smallest singular value of $[Z]$ [3], and the

determinant of $[Z]$ [5], which, however, is not directly applicable to non-square matrices. In a typical analysis scenario, the singularity measure is sampled on a sufficiently fine grid of $k_\rho R$, yielding a graph like the one shown in Fig. 1a, or Fig. 2 in [3]. The cut-off wave numbers, which are at the first zeros of the

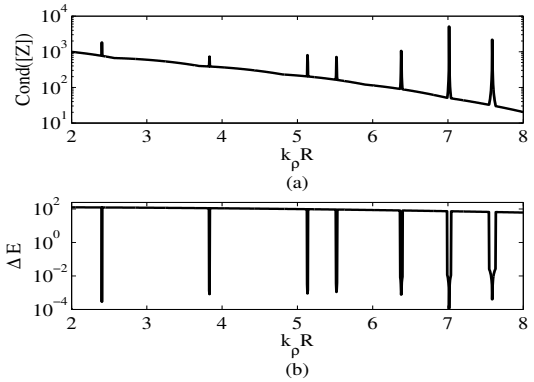

Figure 1: Singularities at the zeros of the Bessel functions. For this graph, $N = 20$ and $\alpha = 1.5$. A very fine sampling grid of 1500 points was needed to reveal all the singularities.

Bessel functions, can be clearly seen as peaks of the matrix condition number.

It is interesting to note that the matrix condition number is quite high *between* the peaks. The high condition number is not due to the existence of a mode, but to the existence of a continuum of approximate spurious solutions to (1). These solutions consist of sources of equal magnitude and alternating sign, that generate fields strongly confined to the vicinity of the sources. Because their E_z field is small on the waveguide boundary, they approximately solve (1), and this is reflected by the high condition number.

The difference between a true mode and a spurious solution, is that while both have vanishingly small fields on the boundary, the fields of the spurious solution are also vanishingly small within the boundary. To distinguish between the two, we define a normalized error measure, ΔE as

$$\Delta E = \frac{\mathrm{rms}([Z]\vec{I})}{\mathrm{rms}([\tilde{Z}]\vec{I})}, \tag{3}$$

where $[\tilde{Z}]$ is an impedance matrix that maps the amplitude vector $\vec{I}$ to the values of E_z at a number of sampling points inside the waveguide. The points can be arranged, for example, on a rectangular grid of reasonable density. In (3), the 2-norm, or root-mean-square value, is denoted by rms( ). To evaluate ΔE, the vector that solves (1) in the least-squares sense is found by a singular value decomposition. The value of ΔE for $\vec{I}$ found at every $k_\rho R$ of Fig. 1a, is shown in Fig. 1b, and it confirms that although the matrix is rather singular between the peaks, there are no modes there.

We now turn to take a closer look at the singularities shown in Fig 1. Zooming in on the first of these singularities, we see in Fig. 2, that it is very sharp and discontinuous. This behavior has undesirable consequences. Because of the discontinuity, there can be no efficient search algorithm to find the singularities. There is simply no indication that a point near a singularity is in fact close, unless it is closer than the discontinuous edges, and the only option is to sample the measure of singularity on a fine grid. The width of the singularity determines the appropriate sampling resolution, and as seen in Fig. 2, the width depends on the number and location of the sources. Note that a small change in these parameters is enough to shrink the singularity considerably. If the sampling grid is kept constant while the number of sources is increased, the singularity may shrink to the point where it falls between grid points and goes undetected. As it is often essential to verify that the results are correct by increasing the number of sources or changing their positions slightly, this lack of reliability in the detection is a serious drawback.

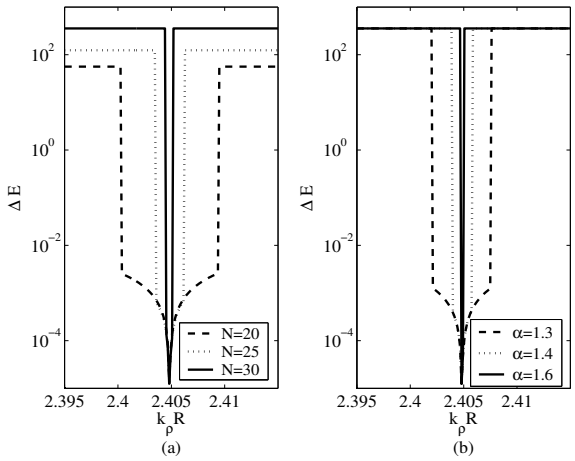

Figure 2: Dependence of the shape of the singularity on (a) the number of sources and (b) the distance from the waveguide boundary. In (a), $\alpha = 1.5$, and in (b), $N = 30$.

3 Spurious Solutions

As we will show in this section, the difficulties discussed above stem from solutions to (1), in which the current filaments are all equal in amplitude, but alternating in sign. To gain further insight into this configuration, we approximate it by a z-directed cylindrical current sheet, of radius ρ_0, carrying a unit-amplitude, circularly-harmonic current, $\exp(jn\phi)$. Here, $n = N/2$ and $\rho_0 = \alpha R$. The longitudinal electric field, E_z, in the region $\rho < \rho_0$, due to this current is given

by

$$E_z = -\frac{\pi\rho_0 k_\rho^2}{2\omega\epsilon_0} J_n(k_\rho\rho) H_n^{(2)}(k_\rho\rho_0) e^{jn\phi}; \qquad \rho < \rho_0, \tag{4}$$

where J_n is the nth order Bessel function and ϵ_0 is the free-space permittivity. When $n >> k_\rho\rho_0$, the spatial variation of the current is fast on a radial-wavelength scale, and E_z can be approximated by

$$E_z \approx \frac{k_\rho^2\rho_0}{2j\omega\epsilon_0 n}\left(\frac{\rho}{\rho_0}\right)^n e^{jn\phi}; \qquad \rho < \rho_0. \tag{5}$$

This shows that if the spatial variation of the current is rapid enough, its field will be very small even when the observation point is quite close to the current distribution.

The behavior seen in Figs. 1 and 2 can now be explained. The slope from which the singularities protrude in Fig. 1a is due to the described spurious solutions. From (5), we see that when k_ρ increases, the E_z field of the spurious solution, which is its absolute boundary condition error, increases, and consequently, the matrix condition number decreases. This also explains the gradual broadening of the peaks at the right end of the figure.

As to Fig. 2, if for a fixed α, the number of sources is increased, it would be like increasing n in (5), and if for a fixed N, α is increased, it would be like increasing ρ_0 in (5). In both cases, the absolute error of the spurious solution would decrease, contracting the singularity. To keep the singularities wide enough, one should therefore use as few sources as possible and they should be placed as close as possible to the boundary. While this facilitates the detection of the singularities, the accuracy of the field approximation is bound to suffer. As we show in the next section, the need to strike a delicate via media between these conflicting goals is obviated by the proposed method.

4 A Spurious-Free SMT Formulation

As explained in Section 2, it is the normalized error, ΔE, which takes into account also field values inside the waveguide, that reliably indicates the existence of a true mode. Hence, instead of evaluating ΔE for the least-squares solution of (1), it would be better to find the vector that minimizes ΔE for a given $k_\rho R$, and then use this minimum value as the measure of singularity. Direct differentiation shows that the stationary vectors of ΔE are the generalized eigenvectors of the following generalized eigenvalue problem

$$[Z]^\dagger[Z]\vec{I} = \xi[\tilde{Z}]^\dagger[\tilde{Z}]\vec{I}. \tag{6}$$

The generalized eigenvector $\vec{I}_{\min}$, which corresponds to the minimum generalized eigenvalue, $\xi_{\min}$, yields the minimum ΔE, which is simply $\sqrt{\xi_{\min}}$. When $k_\rho R$ is a cut-off wave number, the field due to $\vec{I}_{\min}$ indeed approximates a true mode, but the advantage of this scheme is that $\vec{I}_{\min}$ and $\xi_{\min}$ change continuously when moving from one singularity to the next.

The generalized eigenvalue decomposition can be carried out by a number of methods quite efficiently, i.e., without a significant increase in the computation time relative to any of the other measures of singularity. In this example, we used Van Loan's algorithm for the generalized singular value decomposition (GSVD) [6].

To demonstrate the effectiveness of the spurious-free formulation, the plots of Figs. 1 and 2 were recalculated with the same N and α using the GSVD. The results are shown in Figs. 3 and 4, respectively. The slope from which

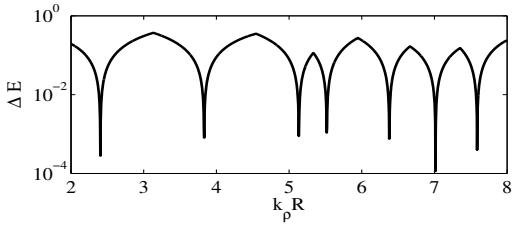

Figure 3: Singularities at the zeros of the Bessel functions, calculated with the spurious-free SMT formulation. For this graph, $N = 20$ and $\alpha = 1.5$. The sampling grid is the same as that of Fig. 1, although a much coarser grid could have been used.

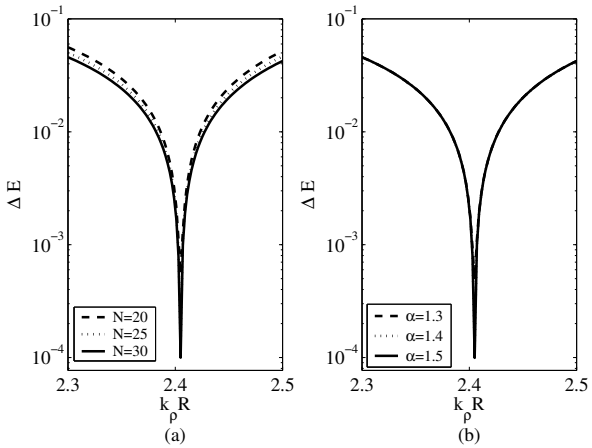

Figure 4: The spurious-free SMT formulation. Dependence of the shape of the singularity on the number of sources (a) and the distance from the waveguide boundary (b). In (a), $\alpha = 1.5$, and in (b), $N = 30$. Note that the range of the abscissa is ten times that of Fig. 2.

the singularities protruded in Fig. 1 has disappeared in Fig. 3, and the curve is simply a superposition of all the true singularities. The minima of the curve can be found with far less iterations: a sampling grid of 75 points suffices to show

all the singularities clearly (1500 points were needed in Fig. 1). After these are found approximately, a line-search algorithm can be applied to find the cut-off wave numbers with high accuracy.

As seen in Fig. 4, the high sensitivity of the width of the singularity to the location and number of sources has been eliminated, making it highly improbable that a singularity should go undetected.

5 Summary

The difficulties in SMT-based waveguide mode determination have been explained by the existence of spurious solutions in ordinary formulations. A spurious-free formulation has been presented and shown to render the method more reliable and efficient. These improvements could pave the way for more widespread use of SMT in waveguide mode determination, correspondent with its recognition in the field of scattering problems.

Acknowledgment

We would like to thank Dori Peleg for pointing out the connection between the minimization of ΔE and the generalized eigenvalue decomposition.

References

[1] D. I. Kaklamani and H. T. Anastassiu, "Aspects of the method of auxiliary sources (MAS) in computational electromagnetics," *IEEE Antennas and Propagation Magazine*, vol. 44, no. 3, pp. 48–64, June 2002.

[2] C. Hafner, *The Generalized Multipole Technique for Computational Electromagnetics*. Norwood, MA: Artech House, 1990.

[3] D. L. Young, S. P. Hu, C. W. Chen, C. M. Fan, and K. Murugesan, "Analysis of elliptical waveguides by the method of fundamental solutions," *Microwave and Optical Technology Letters*, vol. 44, pp. 552–558, Mar. 2005.

[4] A. Hochman and Y. Leviatan, "Modal dynamics in hollow-core photonic-crystal fibers with elliptical veins," *Opt. Express*, vol. 13, pp. 6193–6201, Aug. 2005.

[5] Z. Altman, H. Cory, and Y. Leviatan, "Cutoff frequencies of dielectric waveguides using the multifilament current model," *Microwave and Optical Technology Letters*, vol. 3, no. 8, pp. 294–295, Aug. 1990.

[6] C. F. Van-Loan, "Generalizing the singular value decomposition," *SIAM Journal on Numerical Analysis*, vol. 13, no. 1, pp. 76–83, Mar. 1976.